Freestanding doubly open-ended TiO₂ nanotubes for efficient photocatalytic degradation of volatile organic compounds

Seunghyun Weon [a,1], Jongmin Choi [b,1], Taiho Park [b,*], Wonyong Choi [a,b,*]

[a] Division of Environmental Science and Engineering, Pohang University of Science and Technology (POSTECH), Pohang, 37673, Republic of Korea
[b] Department of Chemical Engineering, Pohang University of Science and Technology (POSTECH), Pohang, 37673, Republic of Korea

A R T I C L E   I N F O

A B S T R A C T

We synthesized freestanding doubly open-ended TiO₂ nanotubes (DNT) film and compared their photocatalytic activity and durability during the repeated degradation cycles of volatile organic compounds (VOCs) with those of TiO₂ nanotubes (TNT) film. DNT exhibited higher activity and durability for the photocatalytic degradation of gaseous acetaldehyde and toluene than TNT. The doubly open-ended structure of DNT allows O₂ molecules to be easily supplied to the active sites, which increases not only the intrinsic photocatalytic activity but also the resistance to catalyst deactivation. The freestanding DNT film was additionally loaded with TiO₂ nanoparticles (NP@DNT) in the inner wall to further increase the activity for VOC degradation. The photocatalytic activity of NP@DNT was higher than bare DNT and bare TNT by 1.3 and 1.8 times, respectively. Unlike the case of DNT, the TiO₂ nanoparticles loaded TNT (NP@TNT) exhibited a lower activity than bare TNT, probably because the TiO₂ nanoparticles blocked the TNT channels with hindering the mass transfer of O₂ and VOC molecules. DNT with doubly open-ended structure serves as a versatile platform of fabricating nanostructured photocatalysts with maintaining the open channel structure that facilitates the mass transfer of O₂ and VOC molecules.

1. Introduction

As people spend most of their time in indoor environment, the indoor air quality (IAQ) emerged as one of the crucial concerns [1]. Volatile organic compounds (VOCs) are major pollutants in indoor environment, which induce adverse effects on human health such as excessive fatigue, headache, skin trouble, and sick building syndrome [2,3]. The conventional methods to remove VOCs are adsorption by activated carbon [4], filtration [5], and thermal oxidation [6]. However, the removal by adsorption and filtration generates secondary wastes and the thermal oxidation requires high temperature [7]. Because of these drawbacks, cost-effective methods that completely degrade VOCs are being sought for air purification. Photocatalytic oxidation is an ideal method for removing VOCs that are present in indoor environment because photocatalysts degrade VOCs to harmless carbon dioxide and water and operate even in ambient temperature and pressure [8–14].

Titanium dioxide (TiO₂) is a popular photocatalyst for environmental remediation because of abundance and low material cost, outstanding chemical and photochemical stability, and high capacity for photooxidation [15–17]. Despite its excellent photooxidation power, TiO₂ photocatalyst suffers from the catalyst deactivation which is induced by the accumulation and strong adsorption of recalcitrant carbonaceous intermediates at the catalyst active sites as a result of incomplete degradation of VOCs [18–20]. Since the formation of carbonaceous deposits is often caused by an insufficient supply of O₂, facilitating the transport of O₂ molecules onto the catalyst active sites can retard the deactivation process. In our recent study [21], it was demonstrated that TiO₂ nanotubes (TNT) with open channels facilitate the diffusion of O₂ molecules to the active sites and exhibit a higher resistance to the catalyst deactivation in comparison with the TiO₂ nanoparticles film. As a result, the intensity of carbon deposit signal (measured by secondary ion mass spectrometry) was indeed much reduced on TNT film. Designing an open structure that allows facile O₂ diffusion seems to be a critical strategy for the development of efficient photocatalysts for VOCs degradation.

Recently, freestanding doubly open-ended TiO₂ nanotubes (DNT) film attracted much attention because of the unique both-side-open structures [22–24]. Unlike TNT film that is open to the one-side, DNT film with both sides open is removed from the

non-reactive Ti-foil substrate which can be the recombination site of charge carriers and its structure facilitates the diffusion of substrates [25]. Because of its advantages, DNT film has been successfully employed to increase the activity of dye-sensitized solar cells (DSSCs) [26–28]. In this respect, DNT's doubly open-ended tube structure can further facilitate the mass diffusion of O_2 and VOC molecules to active sites of TiO_2 in comparison with TNT, which can increase the photocatalytic activity of VOCs degradation and the resistance to the catalyst deactivation.

This study investigated the potential application of DNT as an air-purifying photocatalyst. The photocatalytic activity and durability of DNT and TNT were compared to demonstrate the superior performance of DNT. DNT film was additionally decorated with TiO_2 nanoparticles (NPs) (NP@DNT) that further increased the photocatalytic activity for VOCs degradation because of the enhanced number of surface active sites. The doubly open-ended structure of DNT seems to be an ideal platform of building nanostructured photocatalysts for efficient VOC degradation.

2. Experimental section

2.1. Synthesis and modification of DNT

Freestanding doubly open-ended TiO_2 nanotubes (DNT) film was prepared by the potentiostatic anodization method [26]. All anodization processes were performed using Ti-foil (99.7%, 0.25 mm, Aldrich, USA) as a working electrode and carbon plate as a counter electrode. Before anodization, the Ti-foil was ultrasonically washed sequentially with acetone, ethanol, and distilled water. Then, the first anodization was conducted at 60 V for 90 min in ethylene glycol solution containing 0.25 wt% NH_4F and 0.3 vol% distilled water at room temperature to produce TiO_2 nanotubes (TNT) on Ti-foil. The resulting sample was ultrasonically cleaned using ethanol to remove the debris, followed by thermal annealing at 250 °C for 2 h. The sample was then anodized one more time under the same anodizing conditions for a short time (5–10 min). After the two-step anodization, the TNT on Ti-foil was immersed in 33 wt% H_2O_2 solution. The H_2O_2 solution removed an amorphous titania fraction generated at the bottom of TNT during the second-step anodization, which had weak chemical stability compared to the thermally annealed TNT. As a result, TNT film was separated from the Ti-foil, and the closed bottom layer of the TNT film became open with increasing the immersion time. The resulting DNT film was cleaned with ethanol and dried in air. The as-prepared amorphous DNT film was then annealed at 450 °C for 30 min with a cover-glass on it, which transformed the amorphous DNT to a crystalline anatase DNT, appearing white in color (step I in Fig. 1).

The DNT film was additionally loaded with TiO_2 nanoparticles (NP@DNT) in the inner wall to further increase the active surface area. Compared with the previous method that loaded TiO_2 NPs on DNT film on FTO substrate for solar cell application [28], a new procedure was developed in this work with optimizing various parameters to fabricate a freestanding NP@DNT film as illustrated in Fig. 1a. The crystallized (anatase) DNT film was immersed in an acidic aqueous solution containing $TiCl_4$ (0.2 M) and heated at 70 °C for 60 min to induce the formation of TiO_2 NPs with a few-nm in size on the inner wall of the DNT film (step II). Since the rapid formation of TiO_2 NPs may result in the agglomerate formation, maintaining the optimal temperature and reaction time (70 °C for 60 min) was critical. The intrinsic color of $TiCl_4$ solution (0.2 M) was transparent. As reaction goes, the color of the solution changed from transparent to sky-blue (around 60 min) and finally changed to white (after 100 min) which might be the signal of aggregation of TiO_2 NPs on the surface of DNT. After loading TiO_2 NPs, the decorated DNT film was washed with ethanol, dried in air, and re-annealed to crystal-

ize anatase TiO_2 NPs to form NP@DNT (step III). The SEM images of the top and bottom surfaces of the fabricated NP@DNT film (Fig. 1b) clearly showed both top and bottom opened-structure of which the diameters are 100 nm and 50 nm, respectively. In addition, the HR-SEM cross-sectional images and TEM images of DNT and NP@DNT films clearly show that the inner channel of NP@DNT is decorated with TiO_2 NPs (Figs. 2 and S1). The NP decoration did not change any crystalline phase of TNT and DNT confirmed by characterizations (XRD, XPS) of each photocatalysts (Figs. S2 and S3). The length of TNT between 8.4 and 17 μm was efficient for VOCs degradation [29], thus NP@DNT films of 15 (±2) μm length were prepared in this study. A TNT film decorated by TiO_2 NPs (NP@TNT) and a TiO_2 NP film directly deposited on a glass plate (NP@glass plate) were also prepared as control samples through a similar procedure and were compared with NP@DNT for the photocatalytic activity.

Loading TiO_2 NPs on a freestanding DNT film was difficult because the freestanding DNT film itself was easily curled and broken during heat treatment which is required for decorating TiO_2 NPs on the surface of DNT. To produce a large-size and flat NP@DNT film, several key steps should be carefully considered during the fabrication procedure. During annealing step, the rough top-surface of DNT (Fig. 3a) induced different thermal expansion which caused a curling of the DNT film. To minimize such problem, bottom-up annealing (flipping DNT surface over) and appropriate pressure are required (Fig. 3b and c). A proper pressure (4 Pa) was easily applied on the DNT film by cover glass. The washing step is also a crucial factor to prevent curling, because the capillary force exerted a bending moment on the DNT. The bending moments of nanotubes are governed by the surface tension of employed solvent, and a low surface tension of solvent is critical to minimize the curling problem. Ethanol is a proper solvent for washing step because of its low surface tension compared with water (Fig. 3d).

For comparison with DNT and NP@DNT, Pt-loaded and Ag-loaded TiO_2 were obtained using a photodeposition method. An aqueous suspension of commercial TiO_2 (P25) with an average surface area of $50 m^2 g^{-1}$ and primary particle size of 20–30 nm was irradiated for 30 min with a 200-W mercury lamp in the presence of H_2PtCl_6 (or $AgNO_3$) and methanol (1 M) as an electron donor. The resulting Pt/TiO_2 (Ag/TiO_2) powder was collected by filtration and washed with deionized water. For VOC degradation test, Pt/TiO_2 (Ag/TiO_2) powder were coated on a glass substrate ($1 \times 1 cm^2$) using a doctor-blade method. Photocatalyst powder was mixed with ethanol in a concentration of 0.15 g/mL. The mixed paste was spread on the glass substrate, dried under air and then heated at 200 °C for 2 h to remove residual ethanol.

2.2. Photocatalytic activity measurements

The photocatalytic degradation of acetaldehyde and toluene was conducted in a closed-circulation reactor at ambient conditions. The photocatalyst films of NP@DNT, DNT, NP@TNT, and TNT were prepared in the size of 1 cm × 1 cm and compared for the photocatalytic degradation of VOCs under the same experimental conditions. Since the DNT films were obtained by simply removing the bottom portion of the TNT films on Ti foil, the nanotube lengths of DNT and TNT films were similar and the total surface areas should be similar as well. The glass reactor had a volume of 200 mL, and a quartz window with 3 cm radius. A magnetic bar was placed at the bottom of the glass reactor to circulate the air in the glass reactor. A 370 nm-emitting UV-LED (Luna Fiber Optic Korea, ICN14D-96) was used as a light source. The distance between the UV-LED and the photocatalyst surface was 2.5 cm. The intensity of UV light flux was 10 mW/cm² measured by a power meter (Newport, 1815-C). The glass reactor was connected with a photoacoustic gas monitor (LumaSense, INNOVA 1412i) which could measure the concentrations of toluene, acetaldehyde, acetic acid,
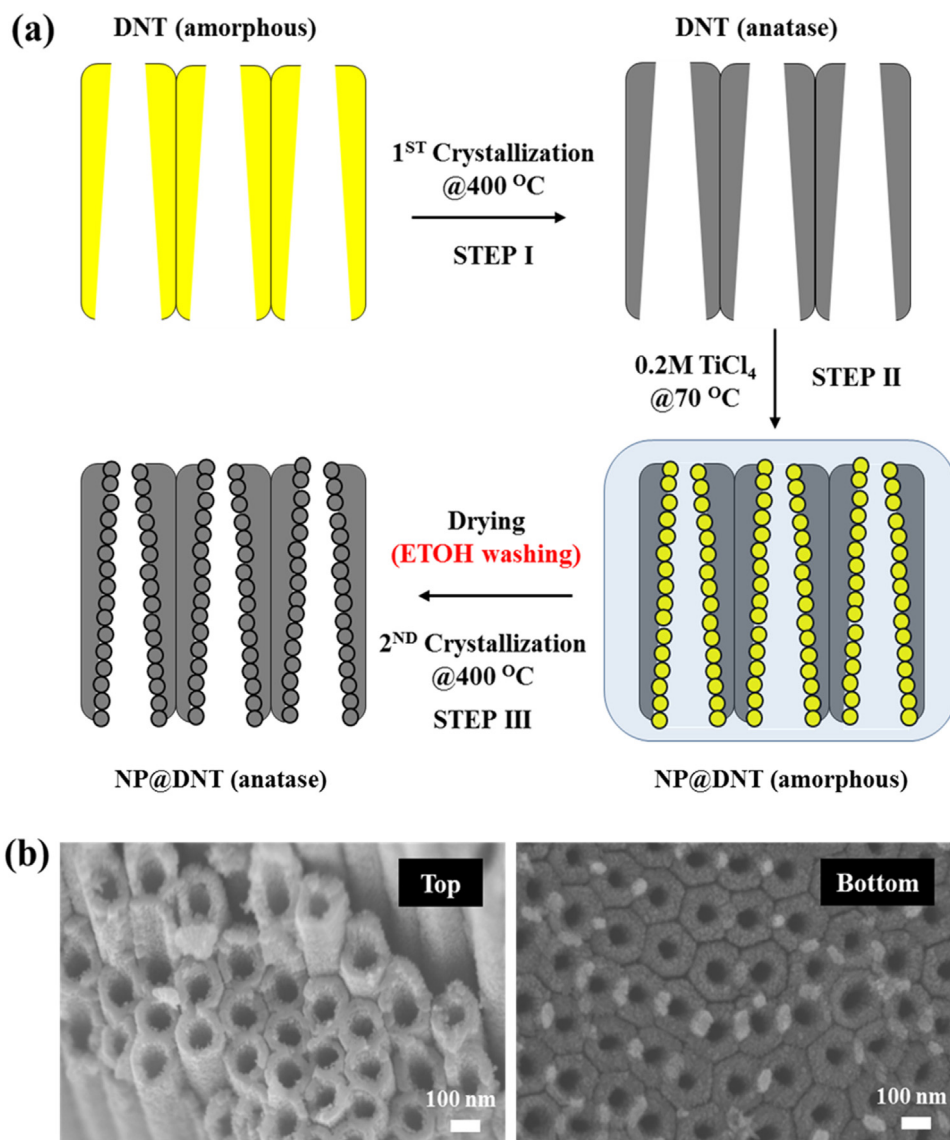
Fig. 1. (a) Schematic illustration of the procedure used to fabricate freestanding DNT film loaded with TiO_2 nanoparticles (NP@DNT). (b) HR-SEM images of NP@DNT.
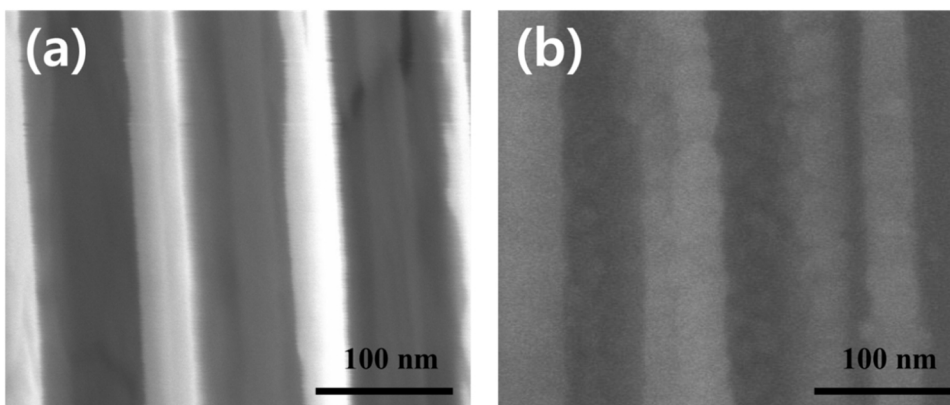

Fig. 2. HR-SEM images of cross-sectional view of (a) DNT film and (b) NP@DNT film.

formaldehyde, carbon monoxide, carbon dioxide, and water vapor. Before each experiment, the glass reactor was purged and filled with high-purity air (20% of oxygen and 80% of nitrogen). All photocatalysts were pre-cleaned by UV illumination for 1 h before each experiment to remove any adsorbed organic impurities. After the cleaning process, the concentration of acetaldehyde and toluene was adjusted by diluting the standard gas (300 ppmv toluene, 1000 ppmv acetaldehyde in Ar) with high-purity air. The typical
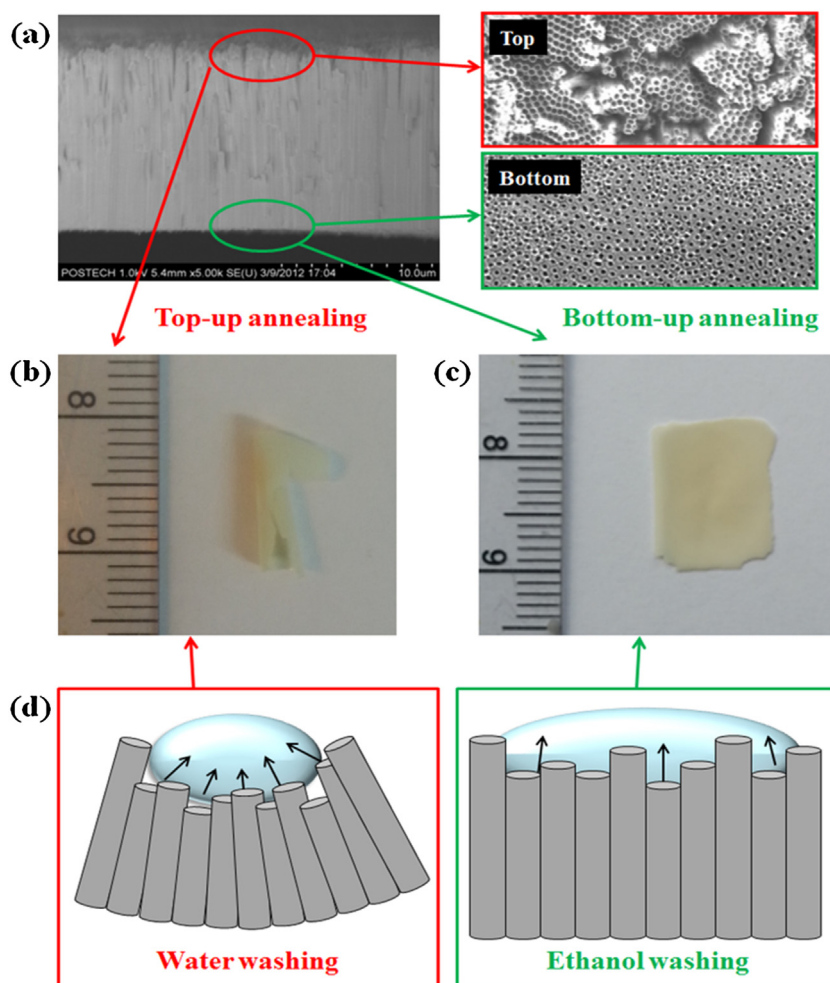
Fig. 3. (a) HR-SEM images of cross-sectional, top, and bottom view of DNT film. Photo image of NP@DNT film fabricated by (b) Top-up annealing and (c) bottom-up annealing. (d) Schematic illustration of the process of changing solvent after decoration step of NP@DNT film.

Table 1
Comparison of the photocatalytic rate constants for the degradation of acetaldehyde and toluene on TNT and DNT photocatalysts.

VOC	Cycle	Pseudo-first order rate constant (10^{-2} min^{-1})			
		TNT	DNT	NP@TNT	NP@DNT
CH$_3$CHO	1	6.19 (±0.43) [0.0609][a]	8.94 (±0.41) [0.0855][a]	4.61 (±0.54) [0.0531][a]	11.39 (±0.92) [0.1154][a]
C$_7$H$_8$	1	6.06 (±0.17)	8.89 (±0.85)	5.17 (±0.27)	10.54 (±0.32)
	2	4.12 (±0.16)	8.53 (±0.74)	4.27 (±0.32)	9.98 (±0.11)
	3	3.64 (±0.15)	8.62 (±0.15)	3.18 (±0.20)	8.56 (±0.28)
	4	3.09 (±0.22)	6.84 (±0.55)	2.60 (±0.39)	8.78 (±0.35)
	5	2.50 (±0.33)	6.52 (±0.81)	1.63 (±0.27)	8.16 (±0.55)

[a] Apparent quantum efficiency for the degradation of acetaldehyde.

inlet concentration of acetaldehyde and toluene was 50 ppmv and 20 ppmv, respectively. The humidity level was regularly monitored by the photoacoustic gas monitor and adjusted at *ca.* 65% by bubbling air through a stainless steel bottle that contained deionized water of which temperature was controlled during the experiment.

2.3. Photoelectrochemical measurements

Photoelectrochemical (PEC) measurements were conducted in a conventional three-electrode system connected to a computer-controlled potentiostat (Gamry, Reference 600). The PEC reactor contained a photoanode, a coiled Pt wire, and an Ag/AgCl/KCl(sat) electrode as a working, a counter, and a reference electrode, respec-

tively; an aqueous solution of 0.5 M Na$_2$SO$_4$ (pH ≈ 6) was used as an electrolyte. For measuring the incident photon-to-current conversion efficiency (IPCE), a 300-W xenon lamp (Newport, 6258) was coupled to a grating monochromator (Newport Cornerstone 260 1/4 M, model 74125) in the wavelength range from 320 to 480 nm, and the light intensity was measured with a UV silicon detector (Newport, 71675). The applied potential was at +0.5 V (*vs.* Ag/AgCl). Both freestanding TNT and DNT films were attached on FTO glass for IPCE measurement. The NT films could be easily detached from the Ti foil by immersion into H$_2$O$_2$ solution and we could get freestanding TNT film (bottom-closed) or freestanding DNT film depending on the etching time duration.
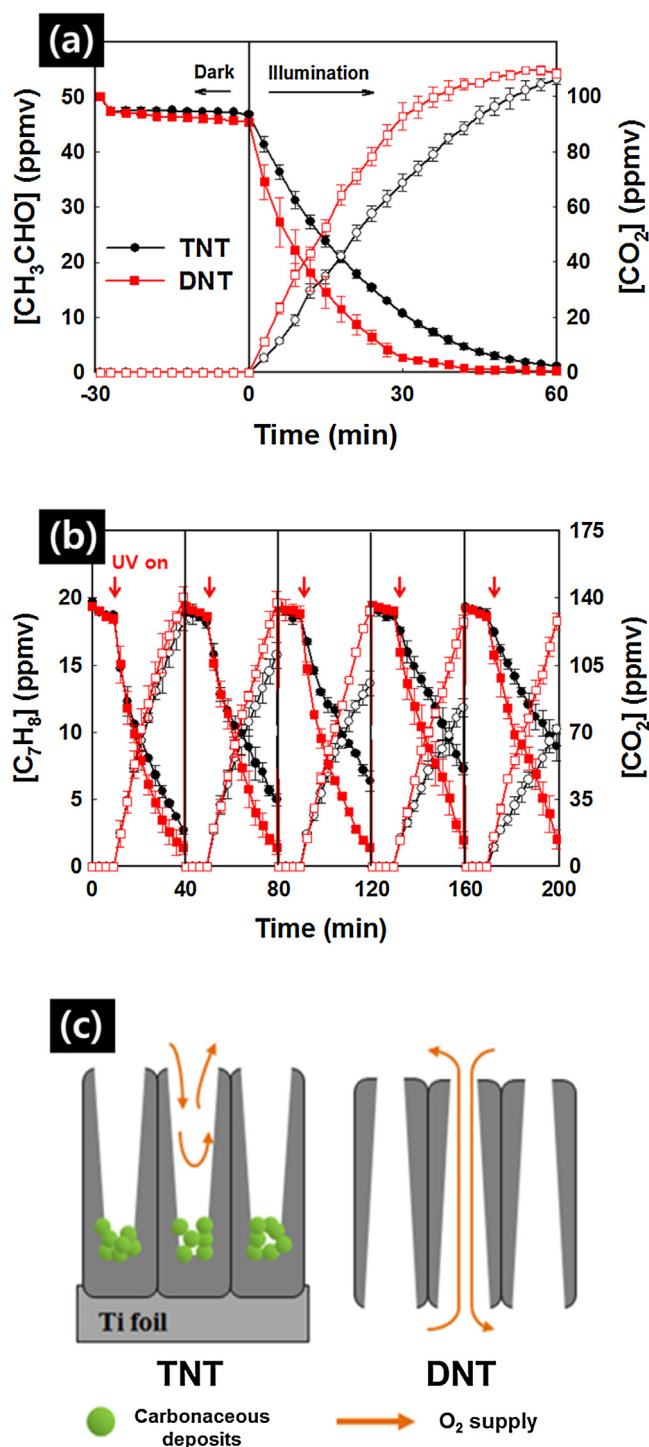
Fig. 4. (a) Photocatalytic degradation of gaseous acetaldehyde on TNT and DNT film. (b) Repeated cycles of photocatalytic degradation of gaseous toluene on TNT and DNT film. (c) Illustration of photocatalytic processes occurring on TNT vs. DNT film. The open symbols represent CO_2 concentration generated from VOC degradation.

2.4. Material characterizations

The morphology of photocatalyst films were measured by field emission scanning electron microscopy (FE-SEM, JEOL, JSM), X-ray diffraction (XRD, Max Science Co., M18XHF) using Cu-Kα radiation, high resolution transmission electron microscopy (HR-TEM, JEOL, JEM-2200FS) with Cs correction. The absorbance of N3 dye solution was measured by a UV/Visible spectrophotometer (Agilent 8453).

3. Results and discussion

The freestanding doubly open-ended TiO_2 nanotubes (DNT) film was prepared by detaching a TNT film from Ti foil [26]. The DNT and TNT films were tested as air-purifying photocatalysts for the degradation of gaseous acetaldehyde and toluene (Fig. 4). Each photocatalysis experiment consisted of a dark circulation period (20–30 min) for adsorption equilibrium and the following irradiation period. Gaseous acetaldehyde and toluene were not degraded at all under 370 nm light illumination in the absence of photocatalysts. The photocatalytic activity of DNT was higher than that of TNT for acetaldehyde degradation under the identical reaction condition. The pseudo-first order rate constants and the apparent quantum efficiency of each photocatalyst for acetaldehyde degradation are summarized in Table 1. The degradation rate on DNT was higher by 1.4 times than that of TNT. The amount of CO_2 generated by complete degradation of acetaldehyde was slightly higher than a theoretical amount of CO_2 because of the decomposition of organic impurities incorporated during TNT fabrication (Fig. 4a). To compare the durability of DNT and TNT films, five successive cycles of photocatalytic degradation of toluene (with an initial concentration of 20 ppmv) were conducted with each photocatalyst film (Fig. 4b). During the photocatalytic degradation of toluene, the possible gaseous intermediates of acetaldehyde, formaldehyde, acetic acid, and carbon monoxide were not detected by the photoacoustic gas monitor within the instrument detection limits. The photocatalytic activity of DNT was maintained during five cycles while that of TNT was progressively reduced (k decreased to ∼40% of initial value after 5th degradation cycle). The outstanding photocatalytic activity and durability of DNT film might be ascribed to the facile mass diffusion of VOC and O_2 molecules through the doubly open-ended channels (see Fig. 4c). Closed-ended structure has a diffusion-limited region in the bottom where O_2 molecules are not rapidly replenished [30]. The fabrication of DNT's doubly open-ended structures removed the bottom part of the tubes that is less accessible to diffusing O_2 molecules and is subject to the deposition of recalcitrant carbonaceous intermediates. The durability of photocatalyst for VOC degradation can be highly related with the supply of O_2 molecules to the active sites of photocatalysts [21]. The TNT film with a closed end can be subject to the accumulation of carbonaceous deposit at the bottom of the tubes where the supply of O_2 molecules and light flux are limited. It has been reported that carbonaceous intermediates such as benzyl alcohol, benzaldehyde, and benzoic acid are complexed with the surface of TiO_2 during the photocatalytic oxidation of toluene, which can cause severe photocatalyst deactivation [31–33]. On the other hand, the doubly open-ended structure of DNT is expected to allow less hindered diffusion of O_2 molecules through the open tubes with significantly retarding the accumulation of recalcitrant carbonaceous intermediates within the channels.

To further increase the photocatalytic activity by increasing the active surface sites, the freestanding DNT film was additionally decorated with a few nm-sized TiO_2 NPs on the inner wall of the channels (NP@DNT). In general, increasing the number of active sites on photocatalysts should increase the photocatalytic degradation efficiency [34,35]. The intrinsic photoactivities of DNT and NP@DNT films were compared with TNT and NP@TNT films by measuring incident-photon-to-current conversion efficiency (IPCE). Higher IPCE values indicate higher photon absorption and higher charge separation efficiency. The IPCE spectra measured as a function of the incident light wavelength (Fig. 5a) clearly showed that NP@DNT and NP@TNT films generate much higher photocurrent than DNT and TNT films because the additionally loaded TiO_2 NPs should absorb more photons. The simple NPs decoration step increased the absorption efficiency of photocatalysts by 3.5 times. To confirm that the TiO_2 NPs loading increases
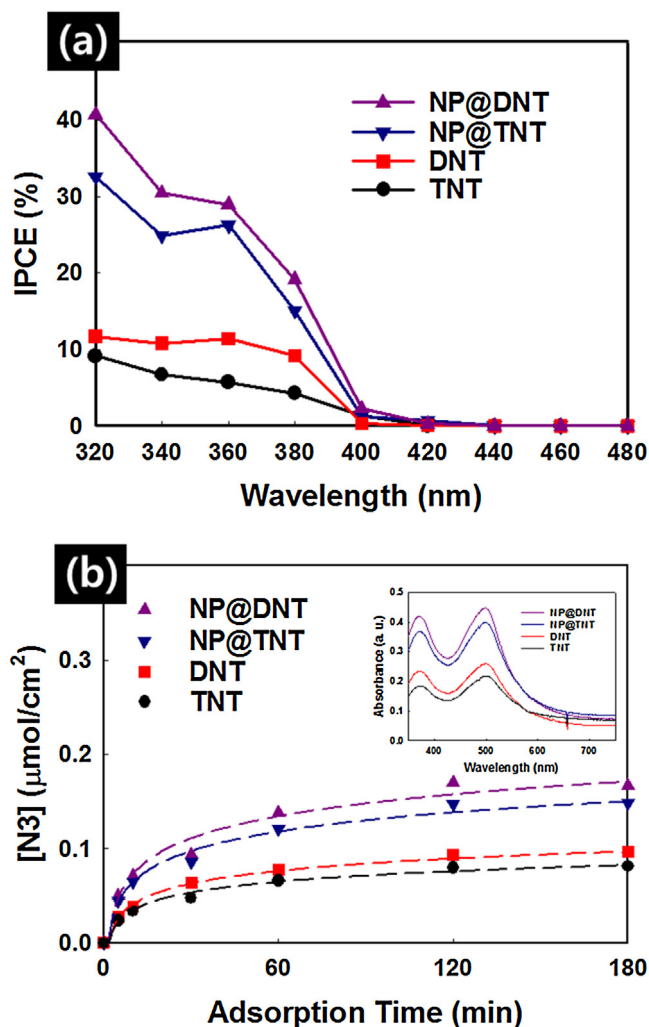
Fig. 5. (a) IPCE spectra of TNT, DNT, NP@TNT, and NP@DNT as a function of the incident light wavelength. The applied potential to IPCE measurement was +0.5 V (*vs.* Ag/AgCl). (b) Amount of adsorbed N3 dye as a function of time. N3 dye solution (0.3 M) was used for adsorption equilibrium on each photocatalyst films ($1 \times 1\,cm^2$). NaOH solution (0.1 M) was used to desorb N3 dye that was pre-adsorbed on the surface of each photocatalyst films.
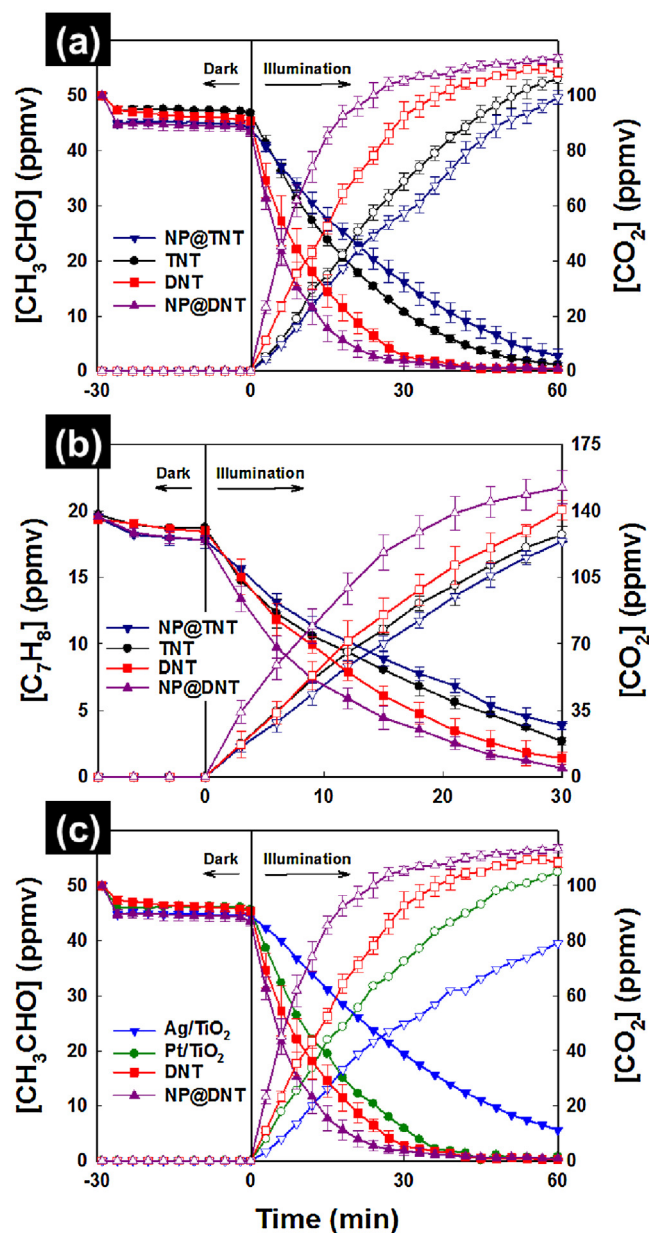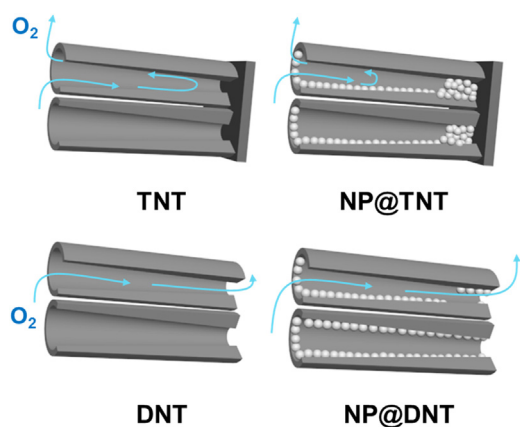

Fig. 6. Photocatalytic degradation of (a) acetaldehyde (aliphatic VOC) and (b) toluene (aromatic VOC) on TNT, DNT, NP@TNT, and NP@DNT. (c) Photocatalytic degradation of acetaldehyde on Ag(1%)/TiO_2, Pt(1%)/TiO_2, DNT, and NP@DNT. The open symbols represent CO_2 concentration generated from VOC degradation.

the number of surface active sites on DNT and TNT films, the adsorption of a dye [N3] was compared among DNT, NP@DNT, TNT, and NP@TNT, which is shown in Fig. 5b. The adsorbed amount of dye for each photocatalyst film was estimated by measuring the absorbance of N3 dye (@540 nm) that was desorbed from the pre-adsorbed film in the presence of 0.1 M NaOH. The adsorption of N3 dye was gradually saturated within 3 h. The adsorbed amounts of dye were little different between DNT ($0.097\,\mu mol\,cm^{-2}$) and TNT ($0.082\,\mu mol\,cm^{-2}$). After decorating the inner surfaces of the DNT and TNT with TiO_2 NPs, the adsorbed amount of dye increased by 72% ($0.167\,\mu mol\,cm^{-2}$) and 82% ($0.149\,\mu mol\,cm^{-2}$), respectively. The simple NPs decoration increased the active sites for adsorption on DNT and TNT films. Both IPCE and dye adsorption measurements consistently indicated that the loading of TiO_2 NPs on DNT and TNT films increased the active surface area.

The effects of TiO_2 NPs decoration on the photocatalytic activity of DNT and TNT for VOC degradation are compared (Fig. 6). During 30 min of dark circulation period, slightly more molecules of acetaldehyde were adsorbed on NP@DNT and NP@TNT than bare DNT and TNT, which supports that the active sites are increased by TiO_2 NPs loading. The photocatalytic activity of NP@DNT was higher than bare DNT by 1.3 times and higher than bare TNT by

1.8 times for the degradation of acetaldehyde (Fig. 6a). The photocatalytic activity of NP@glass plate that was tested as a control was much lower than that of NP@DNT. Unlike NP@DNT, the photocatalytic activity of NP@TNT was lower than bare TNT. The same behaviour was also observed for the photocatalytic degradation of toluene (Fig. 6b). The loading of TiO_2 NPs enhanced the photocatalytic activity of DNT but reduced that of TNT. Five successive cycles of photocatalytic degradation of toluene were conducted using NP@DNT, DNT, NP@TNT, and TNT to test the durability of each photocatalyst film (Fig. S4). The durability of NP@DNT was maintained during five cycles (Fig. S4b) while that of NP@TNT was lower than TNT (Fig. S4a). The inner wall of the TNT structure is hard to be decorated by additional NPs because the nanotubes are attached to the metallic Ti substrate and the bottom side of tubes are closed [25,36]. TiO_2 NPs were aggregated at the closed bottom region during the decoration step of NP@TNT [37]. On the other hand, DNT that

Scheme 1. Schematic illustration of O_2 mass transfer at TNT, DNT, NP@TNT, and NP@DNT.

has doubly open-ended structure can be more easily loaded with TiO_2 NPs on the inner wall with increasing the surface active sites but without clogging the open channel. The structural differences between NP@TNT and NP@DNT (also between TNT *vs.* DNT) and the effect on mass transfer are illustrated in Scheme 1. As a result of the structural difference, the NP@DNT film showed an enhanced photocatalytic activity as an air-purifying photocatalyst compared to bare DNT and NP@TNT. These results imply that not only the higher number of surface active sites but also the aligned open structure for facile mass diffusion is needed to maximize the photocatalytic activity for VOC degradation. Incidentally, DNT and NP@DNT were additionally compared with noble metal loaded titania photocatalysts (*i.e.*, Pt/TiO_2 and Ag/TiO_2) that are commonly employed for the photocatalytic degradation of organic compounds. Fig. 6c shows that both DNT and NP@DNT exhibited higher photocatalytic activity than noble metal-loaded TiO_2 nanoparticulate films, which reconfirms the superiority of DNT structure as an air purifying photocatalyst.

4. Conclusions

In the photocatalytic VOCs removal, both degradation activity and durability of photocatalysts should be considered as important factors. The photocatalyst durability is particularly important for the commercialization of the technology. The doubly open-ended structure of DNT facilitates O_2 molecules to be supplied more efficiently to the active sites in comparison with the close-ended TNT, which retards the generation and accumulation of carbonaceous intermediates. Successful fabrication of DNT film of which inner wall is additionally loaded with TiO_2 NPs was achieved in this work and the resulting NP@DNT demonstrated higher activity and durability for VOC degradation than bare DNT. Unlike NP@DNT, NP@TNT showed a lower activity and durability for VOC degradation than bare TNT probably because the bottom region of TNT was clogged by additional NPs and then O_2 diffusion was further limited. Loading TiO_2 NPs on DNT film increased the surface active sites with maintaining the doubly open-ended structure for facile mass transfer.

Appendix A. Supplementary data

Supplementary data associated with this article can be found, in the online version, at http://dx.doi.org/10.1016/j.apcatb.2016.12.048.

References

[1] M.D. Colton, P. MacNaughton, J. Vallarino, J. Kane, M. Bennett-Fripp, J.D. Spengler, G. Adamkiewicz, Environ. Sci. Technol. 48 (2014) 7833–7841.
[2] S.H. Shin, W.K. Jo, Chemosphere 89 (2012) 569–578.
[3] M.H. Abraham, J.M. Gola, J.E. Cometto-Muniz, Environ. Int. 86 (2016) 84–91.
[4] W.G. Shim, C. Kim, J.W. Lee, J.J. Yun, Y.I. Jeong, H. Moon, K.S. Yang, J. Appl. Polym. Sci. 102 (2006) 2454–2462.
[5] A. Polidori, P.M. Fine, V. White, P.S. Kwon, Indoor Air 23 (2012) 185–195.
[6] K. Everaert, J. Baeyens, J. Hazard. Mater. 109 (2004) 113–139.
[7] F.I. Khan, A. Kr Ghoshal, J. Loss Prev. Process Ind. 13 (2000) 527–545.
[8] J. Mo, Y. Zhang, Q. Xu, J.J. Lamson, R. Zhao, Atmos. Environ. 43 (2009) 2229–2246.
[9] P. Pichat, Appl. Catal. B: Environ. 9 (2010) 428–434.
[10] R. Portela, R.F. Tessinari, S. Suarez, S.B. Rasmussen, M.D. Hernandez-Alonso, M.C. Canela, P. Avila, B. Sanchez, Environ. Sci. Technol. 46 (2012) 5040–5048.
[11] M. Miyauchi, H. Irie, M. Liu, X. Qiu, Yu. Huogen, K. Sunada, K. Hashimoto, J. Phys. Chem. Lett. 7 (2016) 75–84.
[12] X. Zhu, D. Chang, X. Li, Z. Sun, X. Deng, A. Zhu, Chem. Eng. J. 279 (2015) 897–903.
[13] H. Sun, B. Dong, G. Su, R. Gao, W. Liu, L. Song, L. Cao, Appl. Surf. Sci. 343 (2015) 181–187.
[14] A.H. Mamaghani, F. Haghighat, C.S. Lee, Appl. Catal. B: Environ. 203 (2017) 247–269.
[15] M.R. Hoffmann, S.T. Martin, W. Choi, D.W. Bahnemann, Chem. Rev. 95 (1995) 69–96.
[16] H. Park, Y. Park, W. Kim, W. Choi, J. Photochem. Photobiol. C 15 (2013) 1–20.
[17] H. Park, H.-i. Kim, G.-h. Moon, W. Choi, Energy Environ. Sci. 9 (2016) 411–433.
[18] I. Dhada, P.V. Nagar, M. Sharma, Ind. Eng. Chem. Res. 54 (2015) 5381–5387.
[19] S.O. Hay, T. Obee, Z. Luo, T. Jiang, Y. Meng, J. He, S.C. Murphy, S. Suib, Molecules 20 (2015) 1319–1356.
[20] L. Ren, M. Mao, Y. Li, L. Lan, Z. Zhang, X. Zhao, Appl. Catal. B: Environ. 195 (2016) 303–310.
[21] S. Weon, W. Choi, Environ. Sci. Technol. 50 (2016) 2556–2563.
[22] S.P. Albu, A. Ghicov, J.M. Macak, R. Hahn, P. Schmuki, Nano Lett. 7 (2007) 1286–1289.
[23] D. Wang, L. Liu, Chem. Mater. 22 (2010) 6656–6664.
[24] R. Wong, S. Liu, Y. Ng, R. Amal, AIChE J. 62 (2016) 415–420.
[25] Z. Jing-zhong, B. Yang, Z. Kun, L. Ye, K. Lu, Ceram. Int. 41 (2015) 7235–7240.
[26] J. Choi, S. Park, Y. Kwon, J. Lim, I. Song, T. Park, Chem. Commun. 48 (2012) 8748–8750.
[27] J. Choi, G. Kang, T. Park, Chem. Mater. 27 (2015) 1359–1366.
[28] J. Choi, Y.S. Kwon, T. Park, J. Mater. Chem. A 2 (2014) 14380–14385.
[29] Z. Liu, X.T. Zhang, S. Nishimoto, T. Murakami, A. Fujishima, Environ. Sci. Technol. 42 (2008) 8547–8554.
[30] Y. Zhao, G. Gaur, R. Mernaugh, P.E. Laibinis, S.M. Weiss, Nanoscale Res. Lett 11 (2016) 395.
[31] M. Sleiman, P. Conchon, C. Ferronato, J.M. Chovelon, Appl. Catal. B: Environ. 86 (2009) 159–165.
[32] L. Sun, G. Li, S. Wan, T. An, Chemosphere 78 (2010) 313–318.
[33] Y. Huang, S.S.H. Ho, Y. Lu, R. Niu, L. Xu, J. Cao, S. Lee, Molecules 21 (2016) 56–65.
[34] W. Liang, J. Li, Y. Jin, Build. Environ. 51 (2012) 345–350.
[35] A.O. Ibhadon, P. Fitzpatrick, Catalysts 3 (2013) 189–218.
[36] J. Yun, Y. Ng, S. Huang, G. Conibeer, R. Amal, Chem. Commun. 47 (2011) 11288–11290.
[37] J. Choi, S. Song, G. Kang, T. Park, Appl. Mater. Interfaces 6 (2014) 15388–15394.